A HIGH EFFICIENCY UNIT POWER FACTOR SINGLE-PHASE RECTIFIER

Francisco K. A. Lima[1], Cícero M. T. Cruz[2], Fernando L. M. Antunes[3]
Processing Energy and Control Group, Dept. of Electrical Engineering, Federal University of Ceara
P.O. Box 6001 – 60.455-760 – Fortaleza – CE – Brazil
[1]*klima@dee.ufc.br*, [2]*cicero@dee.ufc.br*, [3]*fantunes@dee.ufc.br*

***Abstract* – This paper presents a single-phase rectifier with low conduction losses due to the fact of employing only two controlled switches. A passive non-dissipative snubber provides a further reduction in the rectifier losses. The snubber allows non-dissipative commutation at the switches within a large range of the input current. The snubber also reduces the rate of current grow during the switches turn on and also the rate of voltage grow during the switches turn off. The performance of the snubber circuit associated with the low conduction losses results in a rectifier with high efficiency. The design, simulation and experimental results of a 3kW rectifier and are shown to access the performance of the proposed rectifier.**

I. INTRODUCTION

In power factor correction one of the most common circuit used is the full bridge diode rectifier associated with a boost converter. This converter is shown in Fig. 1.

Substantial power dissipation occurs in the switch because it is subjected simultaneously high di/dt and full output voltage, during the turn on interval. Besides, the reverse recovery mechanism in the boost diode produces high *di/dt* and high current peak through the switch. Since the switch is specified for high voltage it normally has high conduction resistance. Current always flows through three power semiconductors simultaneously causing appreciable conduction losses.

Converters shown in Figures 2 and 3 have lower conduction losses due to the fact that only one or two semiconductors conduct at the same time during the different stages of operation of the converter. These converters present themselves ideal for applications in high power due to their high efficiency; however, as far as the commutation is concern they show the same problem presented by the circuit of Fig. 1.

The In [5] it is presented the version of the three level rectifier employing lossless passive snubber.

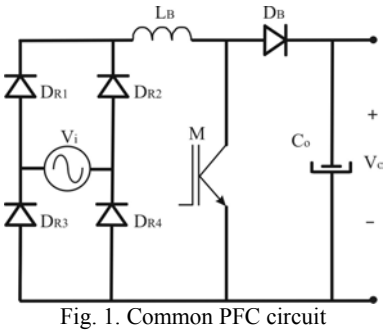

Fig. 1. Common PFC circuit

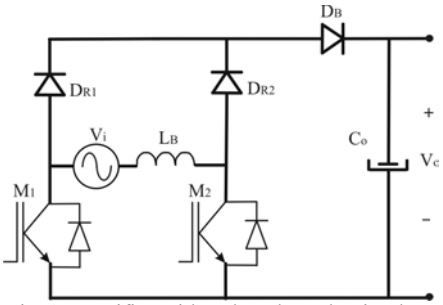

Fig. 2. Rectifier with reduced conduction loss

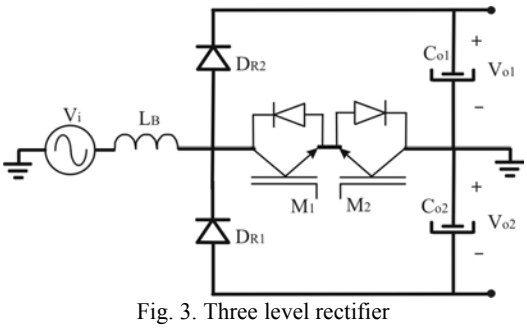

Fig. 3. Three level rectifier

This paper introduces a version of single-phase rectifier with reduced conduction losses and a lossless passive snubber. The single-phase rectifier and the lossless passive snubber are shown in Fig. 4. This converter was presented in [6] and [7], using others techniques of commutation with active components.

Principle of operation and circuit description, design considerations, simulation, experimental results and

conclusion about this converter are described in following sections.

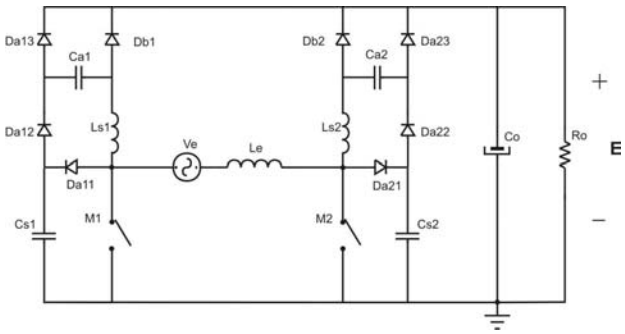

Fig. 4. Voltage single-phase rectifier with a passive lossless snubber

II. PRINCIPLE OF OPERATION AND CIRCUIT DESCRIPTION

In order to show the low conduction losses characteristics of the proposed converter, Fig. 5 shows the stages of operation of the converter without the passive snubber circuit.

Fig.5a shows the 1st stage is the accumulation of energy in the boost inductor L_B in the positive semi cycle of the input voltage.

The 2nd stage shown in Fig.5b represents the transference of energy from the boost inductor to the output stage composed of Co and Ro.

The 3rd and 4th stages shown in Fig.5c and Fig.5d respectively are equivalent to the 1st and 2nd stages but during the negative semi cycle of the input voltage.

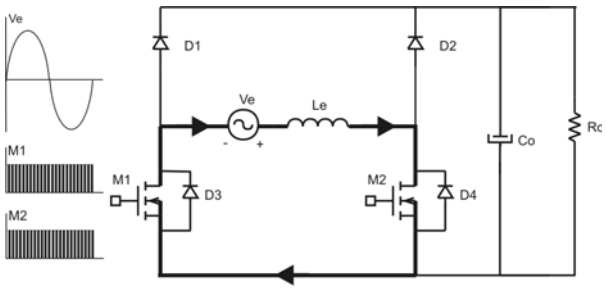

Fig.5a - Stage 1

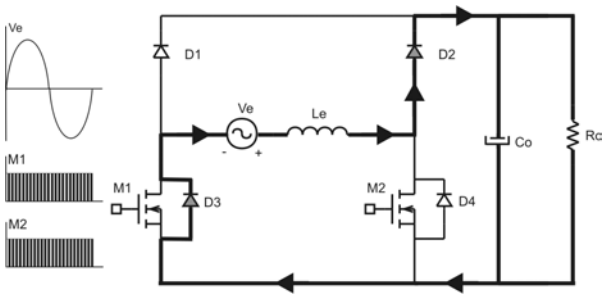

Fig.5b -Stage 2

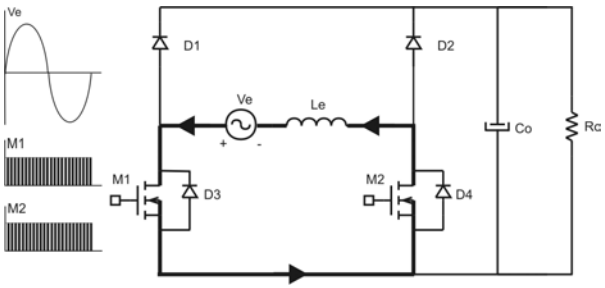

Fig.5c- Stage 3

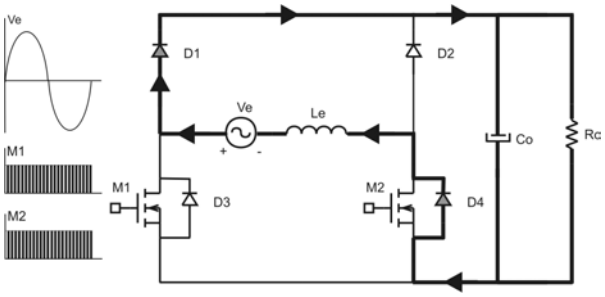

Fig.5d-Stage 4

Fig. 5. Stages of operation

The complete steady state operation of the converter shown in Fig.04 associated with the passive snubber is described in the next stages and circuits for each stage of operation are shown in Fig.6. The following simplifications are made to the commutation stages analysis:

a) input voltage source and boost inductor are represented by a constant current source;

b) output stage is represented by constant voltage sources and all components are ideal.

Stage 1 (t_0-t_1): the input current flows through Db_2, Ls_2 and energy is transferred to the output of the converter.

$$i_L(t) = I, \tag{1}$$

$$V_{Ca}(t) = 0, \tag{2}$$

$$V_{Cs}(t) = V_o, \tag{3}$$

V_o is the output voltage and I is the input current.

Stage 2 (t_1-t_2): at t = t_1 S_2 is turned on and the output voltage is applied to Ls_2, therefore current in Db_2 decreases at linear rate. The S_2 current increases at the same rate.

$$i_L(t) = I - \frac{V_o}{L}t, \tag{4}$$

$$v_{Ca}(t) = 0, \tag{5}$$

$$v_{Cs}(t) = V_o, \tag{6}$$

The time length for this stage corresponds to:

$$\Delta t_2 = \frac{L.I}{V_o}, \tag{7}$$

Stage 3 (t_2-t_3): when the current through Ls_2 equal zero Db_2 turns off, Da_5 turns on and the Cs_2 discharge starts from Vo.

$$i_L(t) = \frac{V_o}{\omega.L}.\text{sen}(\omega.t), \tag{8}$$

$$v_{Cs}(t) = V_o.\frac{\omega_s^2}{\omega^2}.\left[\cos(\omega.t) + \frac{\omega^2}{\omega_s^2} - 1\right], \tag{9}$$

$$v_{Ca}(t) = 0, \tag{10}$$

$$\Delta t_3 = \frac{a\cos\left(1 - \frac{\omega^2}{\omega_s^2}\right)}{\omega.L}, \tag{11}$$

Where

$$\omega = \frac{1}{\sqrt{L.C}},\ C = \frac{C_S.C_a}{C_S + C_a},\ \omega_S = \frac{1}{\sqrt{L.C_S}}, \tag{12}$$

Stage 4 (t_3-t_4): Ls_2 transfer energy to Ca_2. This stage is over when i_{Ls2} equals zero.

$$i_L(t) = \frac{-V_o.\sqrt{2.\omega_s^2 - \omega^2}}{\omega_s^2.L}.\cos(\omega_a.t) + \frac{V_o.\omega_a}{\omega_s^2.L}.\text{sen}(\omega_a.t), \tag{13}$$

$$v_{Ca}(t) = \frac{V_o.\omega_a}{\omega_s^2}.\cos(\omega_a.t) + \frac{V_o.\omega_a}{\omega_s^2}.\text{sen}(\omega_a.t), \tag{14}$$

$$v_{Cs}(t) = 0, \tag{15}$$

$$\Delta t_4 = \frac{a\tan\left(\sqrt{\frac{2.\omega_s^2 - \omega^2}{\omega_a^2}}\right)}{\omega_a}, \tag{16}$$

Where

$$\omega_a = \frac{1}{\sqrt{L.C_a}}, \tag{17}$$

Stages 2, 3 and 4 comprise the turn on snubbing action.

Stage 5 (t_4-t_5): S_2 conducts the input current. In this stage occurs accumulation of energy in the boost inductor.

Stage 6 (t_5-t_6): after S_2 turns off the input current flows through Cs_2 and the voltage across it rises linearly. The voltage on the switch is the same as in Cs_2 with limited dv/dt.

$$V_{Cs}(t) = \frac{I}{C_S}.t, \tag{18}$$

$$\Delta t_6 = \frac{C_S.V_o}{I}.\left(1 - \frac{\omega^2}{\omega_s^2}\right), \tag{19}$$

Stage 7 (t_6-t_7): when V_{Ca2} plus V_{Cs2} equal Vo then Da_6 turns on and Cs_2 begins its discharge.

$$i_L(t) = I.[1 - \cos(\omega_s.t)], \tag{20}$$

$$V_{Cs}(t) = \frac{I}{C_S.\omega_S}.\text{sen}(\omega_S.t) + V_o - V_o.\frac{\omega_a}{\omega_S}, \tag{21}$$

$$\Delta t_7 = \frac{a\,\text{sen}\left(\frac{V_o.\omega_a.C_S}{I}\right)}{\omega_S}, \tag{22}$$

$$V_{Ca}(t_7) = \frac{V_o.\omega_a}{\omega_S}, \tag{23}$$

Stage 8 (t_7-t_8): Da_5 turns on when V_{Cs2} is equal to Vo. One part of the input current flows through Da_4 and Da_5 and another through Ls_2 and Ca_2.

$$i_L(t) = V_o.\frac{\omega_a}{\omega_s}.\sqrt{\frac{C_a}{L}}.\text{sen}(\omega_a.t), \tag{24}$$

$$V_{Ca}(t) = V_o.\frac{\omega_a}{\omega_S}.\cos(\omega_a.t), \tag{25}$$

$$\Delta t_8 = \frac{a\,\text{sen}\left(\sqrt{\frac{L}{C_a}}.\frac{\omega_s.I}{\omega_a.V_o}\right)}{\omega_a}, \tag{26}$$

Stage 9 (t_8-t_9): when i_{Ls2} equals the input current, Da_4 and Da_5 turn off. Ca_2 is discharged at linear rate. The stage finishes the energy remain in the capacitor Ca_2 is transferred to the output.

$$V_{Ca}(t) = -\frac{I}{C_a}.t + \frac{1}{\omega_S}.\sqrt{\frac{C_a.V_o^2.\omega_a^2 - L.I^2.\omega_s^2}{C_a}}, \tag{27}$$

$$\Delta t_9 = \frac{C_a}{I.\omega_s}.\sqrt{\frac{C_a.V_o^2.\omega_a^2 - L.I^2.\omega_s^2}{C_a}}, \qquad (28)$$

Fig. 6 shows the stages of operation for one switching period.

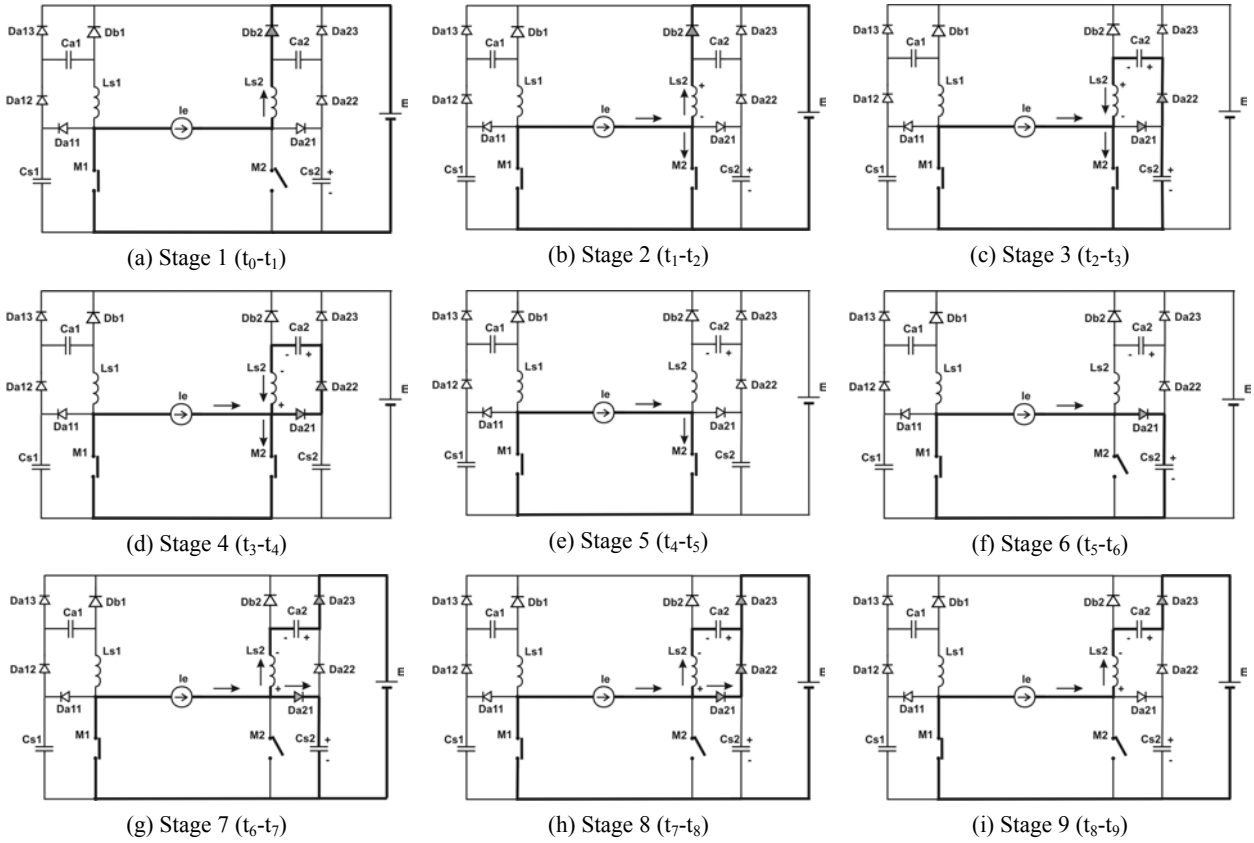

(a) Stage 1 (t_0-t_1) (b) Stage 2 (t_1-t_2) (c) Stage 3 (t_2-t_3)

(d) Stage 4 (t_3-t_4) (e) Stage 5 (t_4-t_5) (f) Stage 6 (t_5-t_6)

(g) Stage 7 (t_6-t_7) (h) Stage 8 (t_7-t_8) (i) Stage 9 (t_8-t_9)

Fig. 6. Stages of operation for commutation analysis

Fig. 7 shows the main waveforms for commutation analysis.

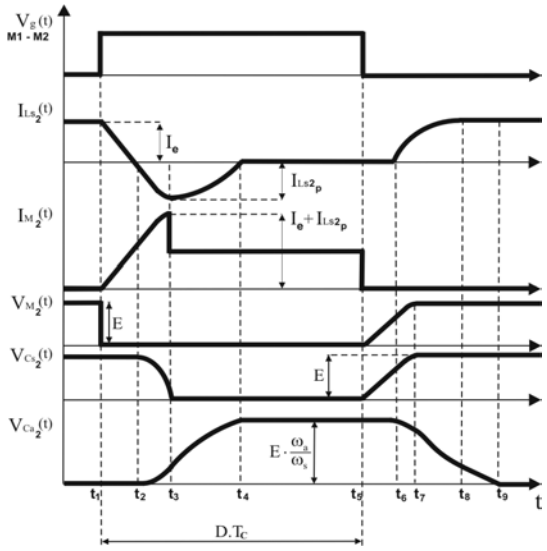

Fig. 7. Waveforms for commutation analysis

III. DESIGN CONSIDERATIONS

A. Considerations for Correct Operation

For the correct operation of the converter according to the stages described above, the passive elements must be designed as following:

- In stage 8(a), the energy accumulated in Ca_2 must to be sufficient to increase the inductor Ls_2 current to the value of the input current, before V_{Ca2} reaches zero. If this condition is not satisfied the converter will reach the topological stage 8(b) depicted in Fig. 8, where soft switching condition at turn on is lost. Hence:

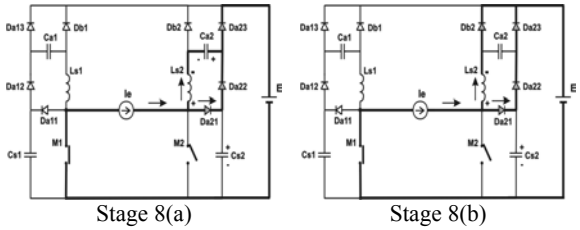

Stage 8(a) Stage 8(b)

Fig. 8. Undesirable stage

$$\frac{1}{2}.C_a.[V_{Ca}(t_7)]^2 > \frac{1}{2}.L.I^2 \ , \tag{29}$$

Substituting (23) in (29), results in:

$$Z_S = \sqrt{\frac{L}{C_{S2}}} < \frac{V_O}{I} \ , \tag{30}$$

For a given value of Z_s impedance defined by (31) the expression (30) will be valid for any input current below the peak value, assuring soft commutation for any value of input current.

$$Z_S = \sqrt{\frac{L}{C_{S2}}} = \frac{V_O}{I_{PK}} \ , \tag{31}$$

I_{Pk} is the peak of sinusoidal input current.

- In stage 7, if the inductor current reaches the input current value before the voltage VCs2 reaches the output voltage, the converter may evolve to stage shown in Fig8(b) and therefore the zero current turn on is lost.

From (20), it is established that the inductor current reaches input current at the angle $\omega_S.t = \pi/2$. Hence, to satisfy the restriction for stage 7 described above, the voltage across capacitor C_{S2} must be lower then output voltage V_o at the angle $\omega_S.t = \pi/2$. Then, from (21):

$$V_o < \frac{I}{C_s.\omega_s} + V_o - V_o.\frac{\omega_a}{\omega_s} \ , \tag{32}$$

$$\frac{V_o}{I.Z_s} < \sqrt{\frac{C_a}{C_s}} , \tag{33}$$

Defining the parameter *x* as the ration between capacitors C_S and C_a, then:

$$x = \frac{C_S}{C_a} \ , \tag{34}$$

In order to ensure soft commutation for a given minimum input current, the parameter *x* is obtained from (35).

$$\frac{I_{\max}}{I_{\min}} = \sqrt{\frac{1}{x}} , \tag{35}$$

The resonant elements are calculated by the (36) and (37).

$$C_s = \frac{1}{Z_s.\omega_s} , \tag{36}$$

$$L = \frac{Z_s}{\omega_s} , \tag{37}$$

B. Time Interval for Snubber Circuit Operation

In PFC the input current and duty cycle are variable during a main cycle, then the time interval available to stages of operation of snubber circuit is limited as function of the input current and duty cycle.

$$\Delta_{ton} = \frac{1}{\omega_s} \cdot \left[\frac{I}{I_{\max}} + \frac{a\cos(-x)}{\sqrt{x+1}} + \frac{1}{x} \cdot a\tan\left(\sqrt{\frac{1-x}{x}} \right) \right] \ , \tag{38}$$

$$\leq T_{sw}.D_{\min}$$

Where T_{sw} is the switching period.

According to (38) the time interval Δt_{on} is proportional to the input current. Hence its maximum value corresponds to the peak input current:

$$\Delta_{ton} = \frac{1}{\omega_s} \cdot \left[1 + \frac{a\cos(-x)}{\sqrt{x+1}} + \frac{1}{x} \cdot a\tan\left(\sqrt{\frac{1-x}{x}} \right) \right] \ , \tag{39}$$

$$\leq T_{sw}.D_{\min}$$

$$\omega_s \geq \frac{\left[1 + \frac{a\cos(-x)}{\sqrt{x+1}} + \frac{1}{\sqrt{x}} \cdot a\tan\left(\sqrt{\frac{1-x}{x}} \right) \right]}{D_{\min}.T_{sw}} \ , \tag{40}$$

The time interval for stages 6, 7, 8 e 9 must be smaller than the smallest conduction time for diode D_{b2} (D_{b1}):

$$\Delta_{toff} = \frac{1}{\omega_s} \cdot \left[\frac{I_{pk}}{I}\left(1-\sqrt{x}\right) + \frac{1}{\sqrt{x}} \cdot a\,\mathrm{sen}\left(\frac{I}{I_{pk}} \right) + \right. \tag{41}$$

$$\left. + a\,\mathrm{sen}\left(\frac{I_{pk}}{I}\sqrt{x} \right) + \sqrt{\frac{1}{x} \cdot \left(\frac{I_{pk}}{I^2}^2 - 1 \right)} \right]$$

$$\leq T_{sw}.(1-D_{\max})$$

When duty cycle is in its maximum, the input current is in its minimum and the time interval Δt_{off} is:

$$\Delta_{toff} = \frac{1}{\omega_s} \cdot \left[\frac{1}{\sqrt{x}} - 1 + \frac{\pi}{2} + \frac{1}{\sqrt{x}} \cdot a\,\mathrm{sen}\left(\sqrt{x}\right) + \frac{1}{x}.\sqrt{1-x} \right] ,$$

$$\leq T_{sw}.(1-D_{\max}) \tag{42}$$

$$\omega_S \geq \frac{\left[\frac{1}{\sqrt{x}} - 1 + \frac{\pi}{2} + \frac{1}{\sqrt{x}} \cdot a\,\mathrm{sen}\left(\sqrt{x}\right) + \frac{1}{x}.\sqrt{1-x} \right]}{T_{sw}.(1-D_{\max})} , \tag{43}$$

The capacitor C_S and inductor L are determined from (36) and (37), using the largest value of the frequency ω_s, obtained from expression (40) and (43).

IV. EXPERIMENTAL RESULTS

Figures 9 to 12 shows the experimental results for output power Po = 3000W, output voltage Vo = 400V, input voltage Vi = 220V and switching frequency fs = 50 kHz.

The passive components used have the following values:

Ls_1 (Ls_2) = 2.55 μH;
Cs_1 (Cs_2) = 10 nF ;
Ca_1 (Ca_2) = 220 nF
L_B = 400 μH.

Figures 13 and 14 shows switch commutation for the minimum input current with guarantees soft commutation.

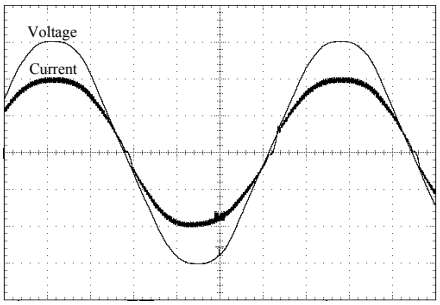

Fig. 9. Input voltage and current waveforms.
Voltage 100V/div, current 10A/div and time 2.50ms/div.

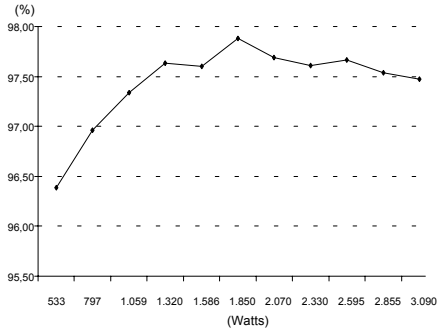

Fig. 10. Output load vs. converter efficiency.

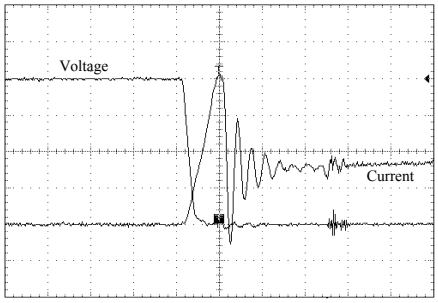

Fig. 11. Turn on commutation in M_2.
Voltage 100V/div, current 10A/div and time 500ns/div.

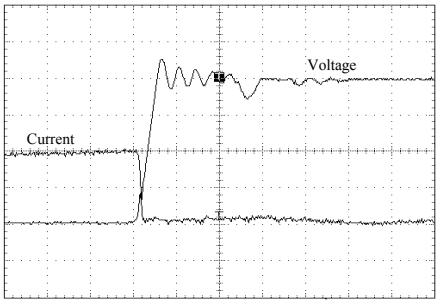

Fig. 12. Turn off commutation in M_2.
Voltage 100V/div, current 10A/div and time 500ns/div.

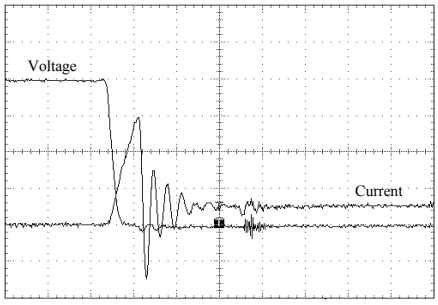

Fig. 13. Turn on commutation in M_2.
Voltage 100V/div, current 10A/div and time 500ns/div.

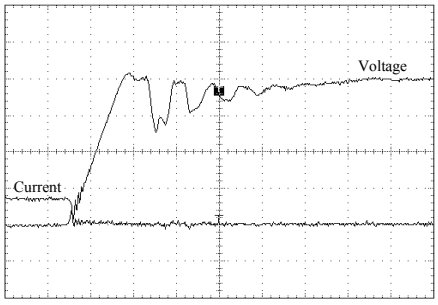

Fig. 14. Turn off commutation in M_2.
Voltage 100V/div, current 10A/div and time 500ns/div.

V. CONCLUSIONS

The results obtained with the proposed PFC circuit associate with a non-dissipative passive snubber lead to the following conclusions:

- The converter operates with unit power factor;
- The commutation losses are very small;
- The converter operates with high efficiency;
- Switches operate with soft commutation.

VI. REFERENCES

[1] L. Duguay, N. Guerrera, M. Ammari, "Novel Boost Converter For Small Power Rectifiers", *INTELEC'97 Coference Records, pp. 132-139*.

[2] R. Y. Fadone, J. M. W. Whiting, "GTO "Taction Chooper with Snubber Energy Recovery", *EPE'93 , Coference Records, pp 276-281*.

[3] C. J. Tseng, C. L. Chen, "Passive Lossless Snubers for DC/DC Converters", *APEC'98 Coference Records, pp 1049-1054*.

[4] A. Pietkiewicz, D. Tollik, "Snubber Circuit and Mosfet Paralleling Considerations fo High Power Boost-Based Power-Factor Correction", *INTELEC'95 Coference Records, pp. 41-45*.

[5] C. M. T. Cruz, I. Barbi, "A Passive Lossless Snubber for the High Power Unidirectional Three-Phase Three-Level Rectifier", *IEEE Industrial Electronics Society*, Vol. 2, Nov. 1999, pp. 909-914.

[6] A. F. Souza, I. Barbi, "A New ZVS- PWM Unity Power Factor with Reduced Conduction Losses", IEEE Transactions on Power Electronics, Vol.10, no. 6, Nov. 1995, pp. 746-752.

[7] A. F. Souza, I. Barbi, "A New ZCS Quasi-Resonant Unity Power Factor with Reduced Conduction Losses", PESC Records, 1995, pp. 1172-1176.